New Representation of Bearings in LS-DYNA®

Kelly S. Carney
Samuel A. Howard
NASA Glenn Research Center, Cleveland, OH 44135

Brad A. Miller
Harding University, Searcy, AR 72143

David J. Benson
University of California San Diego, La Jolla, CA 92093

Abstract

*Non-linear, dynamic, finite element analysis is used in various engineering disciplines to evaluate high-speed, dynamic impact and vibration events. Some of these applications require connecting rotating to stationary components. For example, bird impacts on rotating aircraft engine fan blades are a common analysis performed using this type of analysis tool. Traditionally, rotating machines utilize some type of bearing to allow rotation in one degree of freedom while offering constraints in the other degrees of freedom. Most times, bearings are modeled simply as linear springs with rotation. This is a simplification that is not necessarily accurate under the conditions of high-velocity, high-energy, dynamic events such as impact problems. For this reason, it is desirable to utilize a more realistic non-linear force-deflection characteristic of real bearings to model the interaction between rotating and non-rotating components during dynamic events. The present work describes a rolling element bearing model developed for use in non-linear, dynamic finite element analysis. This rolling element bearing model has been implemented in LS-DYNA as a new element, *ELEMENT_BEARING.*

Introduction

While there are many different types of bearings, all perform the same basic purpose of allowing rotation in one degree of freedom, while constraining motion in the others. Most bearings can also be separated into two major classes: fluid film (or journal) bearings and rolling element bearings. Fluid film bearings are defined by a film of fluid (liquid or gas) separating the rotating and non-rotating components. Fluid film bearings are common in applications such as large industrial steam turbines, industrial compressors, pumps, blowers, and similar types of machines. Rolling element bearings describe a class that includes any bearing with rolling elements (cylindrical, spherical, and conical rollers, balls, and needles for example) separating the rotating and non-rotating components. Rolling element bearings are common in applications such as aeronautic and automotive engines, wheel bearings, gearboxes, and the like. Both classes of bearings have another common feature; they exhibit a non-linear relationship between the relative deflection of the rotating and non-rotating parts, and the load applied. One could say they behave like non-linear springs. Often, but not always, bearings are stiff compared to the structures to which they are connected, or loads are relatively light and therefore, deflections are typically small. In these cases, it can be appropriate to model them with linear load-deflection behavior, i.e. like linear springs. This is a very common practice in rotordynamics and finite elements analysis. However, in the cases where the bearings are soft compared to the surrounding structure, or loads are very large, the non-linearity of the bearings can be very important. The motivation for the current work is to more appropriately model bearings, specifically rolling element bearings, in finite elements models for cases where the non-linear

characteristics are important. Two common examples are aero engine blade-out events and bird ingestion events where the loads on the bearings can be very high. It is anticipated that the resulting non-linear bearing load-deflection model will be useful for other types of analyses as well.

Contact Mechanics for Bearings

In general, rolling element bearings consist of four basic components: rolling elements (commonly spherical balls or cylindrical rollers), an inner ring (or race), an outer ring (or race), and a cage. The function of a bearing is to support radial, axial, and moment loads while providing very low resistance about their axis of rotation. As loads are applied, the inner ring and outer ring move relative to each other, causing the rings to compress one or more of the rolling elements. The races and the rolling elements deform due to the contact pressure at each contact interface. The global load-deflection relationship of the bearing is the composite of the individual contact interface load-deflection characteristics.

For the work he performed in the late 1800's, Hertz (1) is credited with being the first to study what is now referred to as Contact Mechanics - the study of deformable bodies in contact with one another. The stress that develops in the small contact area of two elastic surfaces has come to be known as Hertzian Stress. Others have extended Hertz's work to estimate not only the contact stress, but also the load-deflection relationships in more complicated geometrical contacts. As such, representations of the load-deflection relationship in rolling element bearings are often based on Hertzian stress calculations.

The treatment of contact mechanics in rolling element bearings is not new; in fact, the fundamentals are described in numerous works on the subject of bearings and contact mechanics, some examples of which appear in (2-5). The details of the derivations are left to those texts for the interested reader. However, a short summary is given here to describe the basic concepts as they are applied to the current bearing model. (The treatment can be extended as shown in (6,7) to estimate the stiffness of a ball bearing under a given set of load conditions. This was not done for the current model, but this approach can be used to linearize the model for small perturbations analysis.) Following the treatment by Harris and Kotzalis (3), which is based on Hertz's work and is similar to the other examples, one can generate relationships for the deflection in a contact between two curved bodies, and the normal force applied to push them together. In general, for two curved bodies in contact, the curvature sum and curvature difference are defined respectively as:

$$\sum \rho = \frac{1}{r_{I_1}} + \frac{1}{r_{I_2}} + \frac{1}{r_{II_1}} + \frac{1}{r_{II_2}} \tag{1}$$

$$F(\rho) = \frac{(\rho_{I_1} - \rho_{I_2}) + (\rho_{II_1} - \rho_{II_2})}{\sum \rho} \tag{2}$$

where, in the case of a spherical ball bearing, $r_{I1} = r_{I2}$ = the ball radius, r_{II1}, r_{II2} are the radii of curvature of the race groove in the circumferential and axial directions, respectively.

Consider the contact of the ball and inner raceway in an angular-contact ball bearing shown in Fig. 1. Let body I and II correspond to the ball and the inner race, respectively, and let principal direction 1 coincide with the radial plane and principal direction 2 lie transverse to the direction of rolling. Using these identities,

$$r_{I1} = r_{I2} = \frac{D}{2} \tag{3}$$

$$r_{II1} = \frac{1}{2}\left(\frac{d_m}{\cos\alpha} - D\right) \tag{4}$$

and

$$r_{II2} = f_i D \tag{5}$$

where f is a factor relating the raceway groove depth to the ball diameter and d_m is the nominal bearing pitch diameter. For the outer race contact, r_{I1} and r_{I2} are the same as the inner race contact, but

$$r_{II1} = -\frac{1}{2}\left(\frac{d_m}{\cos\alpha} + D\right) \tag{6}$$

and

$$r_{II2} = -f_i D \tag{7}$$

The initial contact angle, α_0, is the contact angle (as shown in Fig.1) between the balls and the races when the bearing is not loaded. In addition, when not loaded, there may be a clearance, P_d, between the balls and races.

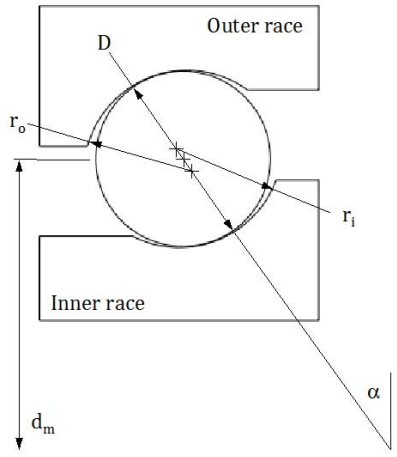

Figure 1. Cross section of a typical angular contact ball bearing, adapted from Harris and Kotzalis (3).

One of the primary assumptions made by Hertz, and thus for the method of Harris and Kotzalis, is that the shape of the contact between the two curved bodies forms an ellipse. With that assumption, the Hertzian formulation gives the curvature difference, Eq. 8, as a function of the semi-major (a) and semi-minor (b) axes of the contact ellipse, and the two complete elliptical integrals of the first and second kind:

$$F(\rho) = \frac{(\kappa^2+1)\mathrm{E}-2\mathrm{F}}{(\kappa^2-1)\mathrm{E}} \tag{8}$$

$$\mathrm{E} = \int_0^{\pi/2}\left[1-\left(1-\frac{1}{\kappa^2}\right)\sin^2\phi\right]^{1/2} d\phi \tag{9}$$

$$\mathrm{F} = \int_0^{\pi/2}\left[1-\left(1-\frac{1}{\kappa^2}\right)\sin^2\phi\right]^{-1/2} d\phi \tag{10}$$

where

$$\kappa = \frac{a}{b} \tag{11}$$

From here, Harris and Kotzalis show that a relationship can be developed between the applied load and the relative approach of the two bodies as:

$$\delta = \frac{2\mathrm{F}}{\pi}\left(\frac{\pi}{2\kappa^2\mathrm{E}}\right)^{1/3}\left[\frac{3Q}{2\sum\rho}\left(\frac{(1-\nu_1^2)}{E_1}+\frac{(1-\nu_2^2)}{E_2}\right)\right]^{2/3}\frac{\sum\rho}{2} \tag{12}$$

where δ= the relative approach of the two bodies in contact (i.e. deflection), Q = applied load, ν_x= Poisson's ratio of material x, E_x = Young's modulus of material x. Equation 12 can be rearranged into the form:

$$Q = K\delta^{3/2} \tag{13}$$

where

$$K = \left[\frac{8\,\pi^2\kappa^2\mathrm{E}}{9\,\Sigma\rho\mathrm{F}^3}\right]^{1/2}\left(\frac{1-\nu_1^2}{E_1}+\frac{1-\nu_2^2}{E_2}\right)^{-1} \tag{14}$$

Equation 14 represents the load-deflection relationship for a single contact (i.e. ball to inner race contact or ball to outer race contact). Various methods exist for solution of the elliptical integrals (E and F), ranging from lookup tables to numerical solutions. One useful approximation is a least squares linear regression developed by Brewe and Hamrock (8) which results in errors on the order of less than 5%.

Now, to determine the composite load-deflection relationship for an entire bearing, Eq. 14 must be applied at each contact (i.e. ball to inner race contact and ball to outer race contact) with the appropriate load for that contact, and summed over all the rolling elements to give the total load-deflection behavior for the bearing.

To determine the load-deflection relationship for each rolling element, consider a single rolling element in a bearing and its contact between the inner race and outer race as shown in Fig. 2. One must apply Eq. 14 to the inner race contact and the outer race contact, such that the total deflection for one rolling element is:

$$\delta_j = \delta_{inner} + \delta_{outer} \tag{15}$$

Where for the j[th] rolling element, $\delta_j$is the total deflection, and δ_{inner}, δ_{outer} are the inner race and outer race contact deflections, respectively.

Substituting Eq. 14 for each race into Eq. 15 and rearranging gives the overall load-deflection relationship for the j[th] rolling element:

$$Q_j = K_{3/2}\delta_j^{2/3} \tag{16}$$

where

$$K_{3/2} = \left[\frac{1}{(1/K_{inner})^{2/3}+(1/K_{outer})^{2/3}}\right]^{3/2} \tag{17}$$

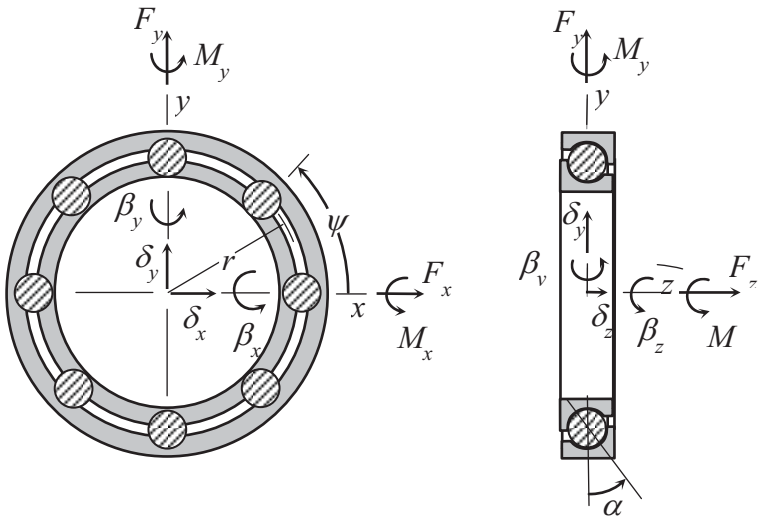

Figure 2. Kinematic model of a ball bearing depicting the inner race degrees-of-freedom and bearing forces.

Ball Bearing Load–Deflection Relationship

Because there are multiple rolling elements in a bearing spaced around the circumference, any applied load is shared unevenly by the rolling elements. It can be shown that the total bearing forces and moments in response to relative displacement between the inner and outer race are found by summing the vector components of the compressive loads and moments from each ball contact, giving

$$\begin{Bmatrix} F_x \\ F_y \\ F_z \end{Bmatrix} = K_{3/2}\sum_{j=1}^{z}\delta_j^{3/2}\begin{Bmatrix} \cos\alpha_j\cos\psi_j \\ \cos\alpha_j\sin\psi_j \\ \sin\alpha_j \end{Bmatrix} \tag{18}$$

and

$$\begin{Bmatrix} M_x \\ M_y \\ M_z \end{Bmatrix} = K_{3/2}\sum_{j=1}^{z} r\delta_j^{3/2}\sin\alpha_j\begin{Bmatrix} \sin\psi_j \\ -\cos\psi_j \\ 0 \end{Bmatrix} \tag{19}$$

Note that the races and the balls have uniform geometry, so the $K_{3/2}$ factor is taken out of the summation. Also, M_z is identically zero in Eq. 19, which indicates that this ideal bearing model allows for free axial rotation of the inner ring.

Implementation in LS-DYNA

The load-deflection relationship established above for a spherical ball bearing is used to develop a non-linear bearing model in LS-DYNA for use in the simulation of dynamic rotating systems. At each time step, the model uses the current relative position of two nodes (representing the centers of the inner and outer races) and calculates a force to generate a new relative position for the next time step, and so on. In this manner, the bearing is represented as a sequence of deflections, and corresponding forces and moments, in the global LS-DYNA model for time transient solutions. The load-deflection behavior is non-linear, and should be more realistic for a bearing subjected to large forces than the more traditional linear spring model. For cases where bearing forces are relatively small, the linear spring model may be preferred to minimize computational times.

Implementation of the non-linear bearing load-deflection model in LS-DYNA is accomplished through the *ELEMENT_BEARING card. The bearing is represented by two nodes, one representing the center of the inner race (usually attached to the rotating part), and the other representing the center of the outer race (usually attached to the non-rotating part). Typically, these two nodes will be coincident when no load is applied (or when only a preload is applied). The user must supply the geometry information in order to calculate a bearing's load-deflection behavior. There are five mandatory cards in *ELEMENT_BEARING. Card 1 defines the bearing ID, type of bearing (currently limited to ball bearing), the two nodes, two coordinate IDs to define the axes of the rotating and non-rotating nodes, and the number of rolling elements. Card 2 defines the Young's modulus and Poisson's ratio for both the rolling elements and the races, and a flag for yield stress limit. (When the yield stress limit is exceeded a message is written to the d3hsp file, and there is no change in the element's behavior.) Cards 3 and 4 are used to define the geometry of the bearing including: the rolling element diameter, bore diameter, outside diameter, pitch diameter, initial contact angle, inner and outer race groove radius to ball diameter ratios, and the bearing clearance. Lastly, card 5 is used to define any preload conditions. There is a preload flag to define the type of preload, and five variables to set either x, y, z displacements and x and y rotations, or x, y, z forces and x and y moments. Refer to Fig. 1 for a description of the geometry variables.

Preload is defined as either a set of forces and moments, or a set of displacements and angles that mimics the preload in a real system. For example, a typical method of providing preload to bearings in a rotor system is to fix the inner race on the rotating shaft by press fit or other mechanical means, while the outer race is constrained radially in the non-rotating structure, but is free to slide axially. Springs are then used to apply an axial preload force to the outer race to prevent the bearings from becoming unloaded and allowing the rolling elements to skid or slide at the contact surface with the races, or becoming overloaded and negatively affecting contact stress. Skidding is detrimental to bearing life, causing local heating, surface damage, galling, increased friction, etc. Therefore, preload is almost always used to apply some nominal contact forces. Preload also affects the load-deflection relationship, so it is important to include it in the bearing model.

Because the bearing load-deflection relationship is non-linear, the stiffness is different depending on the load. Therefore, preload effectively changes the stiffness of a given bearing, such that a preloaded bearing will behave differently than a non-preloaded bearing. To account for this in the DYNA bearing model, the force generated in the bearing is defined as:

$$F_{brg} = \mathcal{F}(\delta_0 + \delta_{node}) - F_{pre} \tag{20}$$

Where δ_{node} is the instantaneous displacement between the two bearing nodes. F_{brg} is the force between the two nodes due to displacement δ_{node}.

To account for the modified stiffness from the preload, one must calculate the force due to the preload displacement (δ_0) combined with the instantaneous displacement between the nodes (δ_{node}), and then subtract the preload force (F_{pre}) as shown in Eq. 20. Notice, because of the non-linearity, this is not equivalent to calculating F_{brg} from the load-deflection relationship directly using δ_{node} as the displacement. In *ELEMENT_BEARING, Eqs. 18 and 19 are implemented to calculate the instantaneous force and moment. If the user supplies preload forces, iteration is required to determine δ_0 from the load-deflection curve, and a Newton-Raphson scheme is used. Alternately, if preload displacements are supplied, F_{pre} is determined directly from the load-deflection relationship. In either case, this calculation is only required once at the beginning of the simulation, as these values are constant for a given analysis. The preload displacement and preload force are considered internal quantities, and are not output as any nodal displacements or forces, they are simply required to ensure the instantaneous forces and displacements are calculated at the correct location on the load-deflection curve. A side benefit of this method is the elimination of the zero force-zero stiffness numerical issues that are possible at zero displacement on the load-deflection curve. Users should take note that if they choose not to provide preload in their analysis, they may encounter numerical instability if their solution involves passing through zero displacement.

Results and Discussion

As a check of the model, a standalone computer program utilizing the same model as developed here has been written in Visual Basic and implemented within Microsoft® Excel to solve Eqs. 18 and 19 for a bearing case with documented results useful for comparison. For comparison purposes with the published results, the model was extended as mentioned above to calculate stiffness from the load-deflection relationship.

To verify the results from the bearing model, the radial and axial ball bearing stiffness coefficients are plotted as a function of radial force and compared to analytical expressions given by Gargiulo (6). Fig. 3 shows the results for a bearing whose design parameters are depicted in Table 1. The radial stiffness represents the case when the initial contact angle is $\alpha_0 = 0$, and the axial stiffness represents the case when $\alpha_0 = 90°$. The differences between the present model and the published results for the radial and axial stiffness coefficients are all less than 3% and 11%, respectively, and the trends match qualitatively.

Table 1. Design Parameters for Bearing Model Comparison Case

Elastic modulus of ball	E_{ball}	207	GPa

Poisson ratio of ball	v_{ball}	0.30	
Elastic modulus of race	E_{race}	207	GPa
Poisson ratio of race	v_{race}	0.30	
Diameter of ball	D	19.1	mm
Bore diameter	D_i	100	mm
Outer bearing diameter	D_o	180	mm
Nominal pitch diameter	d_m	140	mm
Initial contact angle	a_0	40	deg
inner raceway radius to ball diameter ratio	f_i	0.54	
outer raceway radius to ball diameter ratio	f_o	0.52	
Number of balls	z	18	
Clearance	P_d	0.1	μm

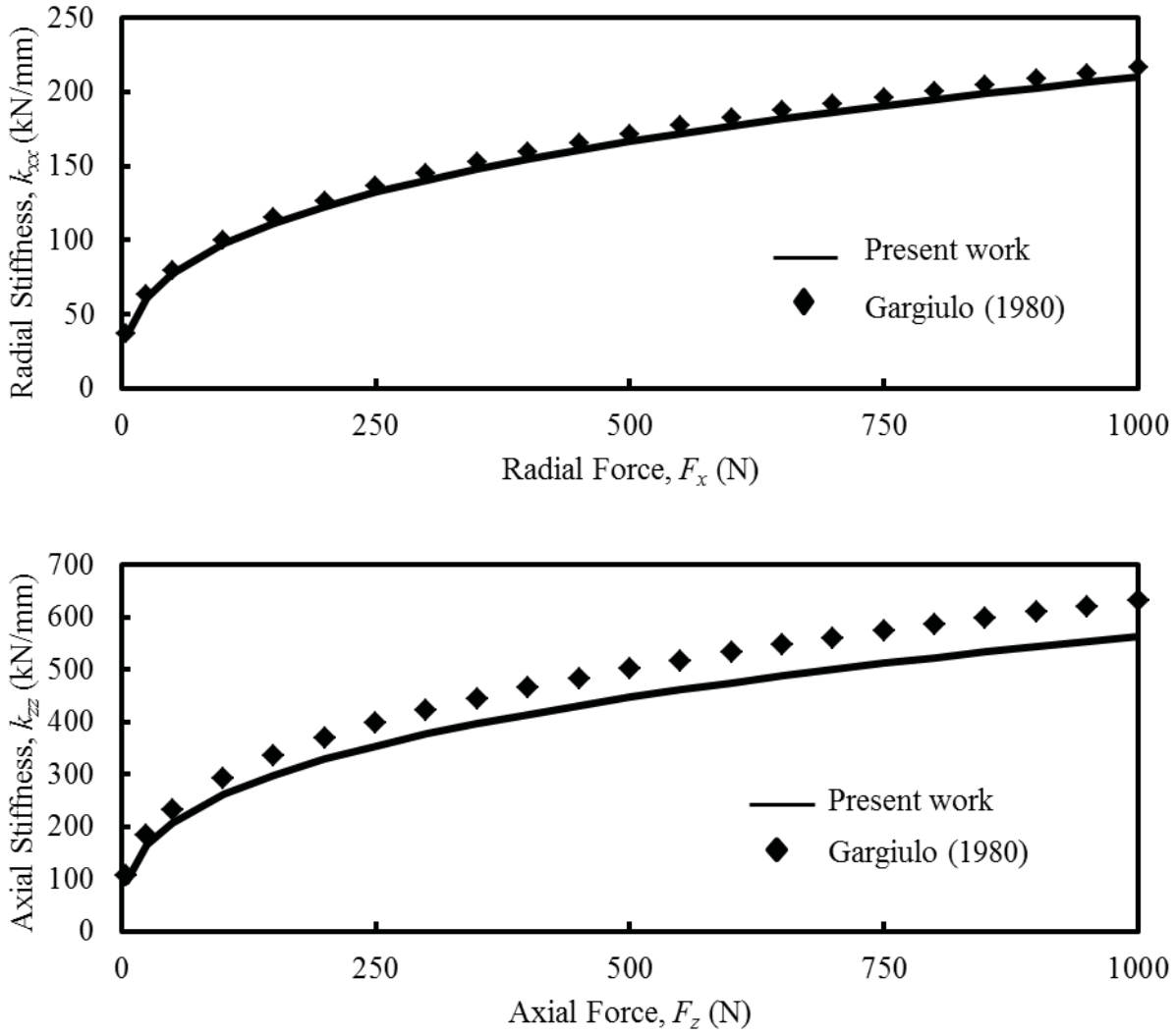

Figure 3. Comparison of the direct radial and axial stiffness coefficients with analytical expressions found in literature.

Conclusions

A nonlinear formulation has been developed relating the bearing forces and moments to the motion of the inner ring in ball bearings. The force-displacement relationships are based on a kinematic model of the inner ring with five degrees of freedom. The model accounts for the elastic deformation of the balls and races near the contact points and neglects the effects of fluid film lubrication and inertia. The model has partially been validated by comparison to closed–form expressions found in literature.

The load-deflection model developed and described herein has been implemented in LS-DYNA as *ELEMENT_BEARING and will be available in the next general release of LS-DYNA. The model is currently only developed for ball bearings, but future work is planned to extend the model to roller bearings and potentially other bearing geometries as needed.

References

1) Hertz, H., "On the Contact of Rigid Elastic Solids and on Hardness," *Miscellaneous Papers*, MacMillen, London, 1896, pp. 163-183.

2) Hamrock, B. J., and Anderson, W. J., "Rolling-Element Bearings," NASA RP 1105, June 1983.

3) Harris, T. A., and Kotzalas, M. N., *Rolling Bearing Analysis, 5th ed., Essential Concepts of Bearing Technology*, CRC Press, Taylor & Francis Group: Boca Raton, FL, 2006.

4) Johnson, K. L., *Contact Mechanics*, Cambridge University Press: Cambridge, 1985.

5) Jones, A. B., *Analysis of Stress and Deflections*, New Departure Engineering Data, Bristol, CT, 1946.

6) Gargiulo, E. P., "A simple way to estimate bearing stiffness," *Machine Design*, Vol. 52, pp. 107-110, 1980.

7) Lim, T. C., and Singh, R., "Vibration Transmission Through Rolling Element Bearings, Part I: Bearing Stiffness Formulation," Journal of Sound and Vibration, Vol. 139 (2), pp. 179 – 199, 1990.

8) Brewe, D. E. and Hamrock. J. J., "Simplified solution for elliptical contact deformation between two elastic solids," ASME Journal of Lubrication Technology, Vol. 99 (4), pp. 485 – 487, 1977.